




RESEARCH ARTICLE | AUGUST 04 2023

Highly polarized positrons generated via few-PW lasers

Special Collection: [Relativistic Plasma in Supercritical Electromagnetic Fields](#)

Bing-Jun Li ; Yan-Fei Li  ; Yue-Yue Chen; Xiu-Feng Weng; Xin-Jian Tan; Xin-Jie Ma; Liang Sheng; Hua-Si Hu



Phys. Plasmas 30, 083103 (2023)

<https://doi.org/10.1063/5.0158256>



View
Online



Export
Citation

CrossMark

Articles You May Be Interested In

Comparative study between CW and PW emissions in selective laser melting

Journal of Laser Applications (June 2018)

Three- and four-nucleon bound states in three dimensions, without PW decomposition

AIP Conference Proceedings (February 2012)

0.1-Hz 1-PW Ti:Sapphire Laser Facility

AIP Conference Proceedings (April 2010)

Physics of Plasmas

Features in Plasma Physics Webinars

Register Today!

Highly polarized positrons generated via few-PW lasers

Cite as: Phys. Plasmas **30**, 083103 (2023); doi: [10.1063/5.0158256](https://doi.org/10.1063/5.0158256)

Submitted: 16 May 2023 · Accepted: 13 July 2023 ·

Published Online: 4 August 2023



View Online



Export Citation



CrossMark

Bing-Jun Li,¹ Yan-Fei Li,^{1,a)} Yue-Yue Chen,^{2,b)} Xiu-Feng Weng,³ Xin-Jian Tan,³ Xin-Jie Ma,¹ Liang Sheng,³ and Hua-Si Hu^{1,c)}

AFFILIATIONS

¹Department of Nuclear Science and Technology, Xi'an Jiaotong University, Xi'an 710049, China

²Department of Physics, Shanghai Normal University, Shanghai 200234, China

³Northwest Institute of Nuclear Technology, Xi'an 710024, China

Note: This paper is part of the Special Topic: Relativistic Plasma in Supercritical Electromagnetic Fields.

^{a)}Author to whom correspondence should be addressed: liyanfei@xjtu.edu.cn

^{b)}Electronic mail: yueyuechen@shnu.edu.cn

^{c)}Electronic mail: huasi_hu@xjtu.edu.cn

ABSTRACT

Spin-polarized positron beams have widely been utilized in applications ranging from fundamental physical studies to material processing. Preparing highly polarized positron beams for accurate probing is a long-standing issue. Here, we put forward a method to produce ultra-relativistic polarized positrons with unprecedented purity in a femtosecond timescale employing a few-PW circularly polarized laser pulse. The fully spin-resolved QED Monte Carlo method is used for simulating the two successive QED processes during the interaction, i.e., nonlinear Compton scattering and nonlinear Breit–Wheeler pair production. As the photons emitted in a circularly polarized laser field are symmetrically polarized, the polarization of the intermediate gamma photon beam averages out to zero, which is advantageous for improving the polarization of positrons. Meanwhile, the moderate laser intensity suppresses the depolarization of the new-born positrons induced by radiation reaction effect. As a result, the polarization of the positrons can reach up to $\geq 90\%$, the highest among the laser-driven polarization schemes conceived hitherto. Furthermore, our method relaxes the requirement on laser intensity to few-PW level, offering a promising way of preparing polarized positrons with current-generation laser facilities.

Published under an exclusive license by AIP Publishing. <https://doi.org/10.1063/5.0158256>

I. INTRODUCTION

Spin-polarized positron beams are a powerful tool in fundamental physical studies and applications, such as improving the sensitivity of the two-photon effect experiments,¹ unraveling nucleon structures,² and testing the standard model or searching new physics beyond it.³ In addition, polarized positrons scattered by materials could provide information on the surface and bulk magnetism of the materials^{4,5} and, consequently, are applied in material processing.

Generally, there are two available means of obtaining polarized positrons. In the first method, unpolarized positrons generated by the Bethe–Heitler process are sent to a storage ring, where the positrons are polarized as a result of radiation due to the Sokolov–Ternov effect.⁶ However, owing to the weak magnetic fields (\sim Tesla), this method requires a rather long polarization time (from tens of minutes to hours),³ huge layout scale, and expenses. Alternatively, polarized positrons can be generated directly using beta decays of specific

radioisotopes⁷ or the Bethe–Heitler process during interactions between circularly polarized gamma rays with a high- Z target. Polarized positrons generated from beta decays cannot be used as beams due to the low density and wide angular divergence. In contrast, positron beams generated by the polarized Bethe–Heitler process are more potential for high-energy physical experiments as proposed in the famous International Linear Collider.^{8,9} However, this method suffers from high depolarization rates and large angular divergences due to multiple scattering in the Coulomb field of nuclei (Mott scattering).^{10,11} To remedy this, the target thickness has to be less than $0.2L_{rad}$,¹² which consequently limits the yield of polarized positrons to $\leq 0.01e^+/e^-$.^{10,13,14} The present available highly polarized (30%–80%) positrons^{13,15–17} at yield $\sim 10^{-4}e^+/e^-$ and angular divergence in the scale of degree still cannot meet the experimental requirements, such as for those at linear colliders.^{8,18} Recently, a large-scale interconnected-undulator-based positron generation system was

conceived, which, however, faces a huge challenge and risk mainly arising from thermal load on the positron production target.¹⁹ Therefore, the ability of efficiently preparing highly polarized positrons is a long-standing issue.

With the rapid development of PW laser technology, schemes employing ultra-intense electromagnetic fields have been proposed to generate polarized positrons in a femtosecond timescale,^{20–24} which exploit two successive strong-field QED processes, nonlinear Compton scattering (NCS) and nonlinear Breit–Wheeler (NBW) pair production. The positrons are polarized at creation due to the asymmetric creation probability between positrons with opposite polarization states. However, this polarization effect averages out to zero in a symmetric oscillating field. Therefore, laser fields with some sort of asymmetric structures are necessary for preventing the cancellation from different half-cycles.^{20,21,23} For instance, polarized positrons can be obtained using a two-color laser pulse²⁰ or a strong unipolar field generated by an ultra-relativistic electron beam propagating in a plasma.²³ However, the polarization degree of positrons in the both methods is limited to $\leq 60\%$. It has been reported in Ref. 21 that the polarization degree can reach 90% by adding a specifically tailored small ellipticity to split two oppositely polarized beams along the minor axis of the laser field. Unfortunately, an improved simulation including the polarization effect of intermediate photons reveals that the average polarization of the positrons in elliptically polarized field is reduced by 35%.²⁴ Replacing the unpolarized seed electrons with polarized ones could make a progress at higher polarization.^{22–24} However, the ability of preparing highly polarized seed electrons (typically $\sim 80\%$ ^{3,13,25}) inhibits the polarization of the produced positrons.

In this paper, we aim to put forward an efficient method of producing highly polarized positrons with polarization degree $\geq 90\%$, higher than any laser-driven schemes conceived hitherto. We use a circularly polarized ultra-intense laser pulse to interact with an unpolarized ultra-relativistic electron beam, as shown in Fig. 1. During the interaction, high-energy photons emitted by seed electrons are well collimated and polarized radially, corresponding to a zero-level average polarization. In the subsequent NBW processes, high-energy photons decay into electron–positron pairs. As for the photon beam with a vanishing average polarization, the degradation effect originating from the photon polarization could be removed. Furthermore, compared with other schemes, typically with laser intensity $\geq 10^{22}$ W/cm², the required laser intensity here is one order of magnitude less, which makes the

depolarization effect of random radiation reaction suppressed, resulting in a high positron polarization degree larger than 90%.

II. SIMULATION METHOD

A recently developed Monte Carlo method²² incorporating all polarization effects in strong-QED processes are employed to calculate the polarization dynamics of electrons, photons, and positrons, during the interaction of a circularly polarized ultra-intense laser pulse with an ultra-relativistic electron beam. This method is based on the fully spin- and polarization-dependent quantum probabilities derived via the Baier–Katkov QED operator method under the local constant field approximation (LCFA), which is valid when the invariant laser field parameter $a_0 \equiv |e|E_0/(m\omega_0) \gg 1$.^{26–28} In LCFA, the photon emission probability and pair production probability are determined by the local value of the quantum parameter, $\chi_{\gamma,e} \equiv |e|\sqrt{-(F_{\mu\nu}p^\nu)^2}/m^3$. Here, $F_{\mu\nu}$ is the field tensor, p^ν is the four-momentum of the photon or electron (positron), E_0 is the laser field amplitude, ω_0 is the laser frequency, and $e < 0$ and m are the electron charge and mass, respectively. Relativistic units $\hbar = c = 1$ are used throughout.

A common stochastic algorithm is employed to describe mechanically the quantum events of photon emissions and pair productions.^{29–32} At each time step Δt , whether a photon (a pair) is emitted (created) is determined by the quantum probability as follows.

The photon emission probability takes the following form:^{28,33}

$$\frac{d^2 W_{\text{rad}}}{dudt} = \frac{C_R}{4} (F_0 + \xi \cdot \mathbf{F}), \quad (1)$$

where $C_R = \alpha m / [\sqrt{3}\pi\gamma_e(1+u)^3]$, α is the fine structure constant, γ_e is the electron Lorentz factor, $u = \omega_\gamma / (\varepsilon_i - \omega_\gamma)$, ω_γ is the emitted photon energy, and ε_i is the electron energy before radiation, respectively. The variables introduced in Eq. (1) read

$$\begin{aligned} F_0 &= -(1+u)\text{Int}K_{\frac{2}{3}}(u') + (u^2 + 2u + 2)K_{\frac{2}{3}}(u') \\ &\quad - u(\mathbf{S}_i \cdot \hat{\mathbf{e}}_2)K_{\frac{4}{3}}(u') - \mathbf{S}_f \left\{ (1+u) \left[\text{Int}K_{\frac{1}{3}}(u') - 2K_{\frac{2}{3}}(u') \right] \mathbf{S}_i \right. \\ &\quad \left. + u(1+u)K_{\frac{1}{3}}(u')\hat{\mathbf{e}}_2 + u^2 \left[\text{Int}K_{\frac{1}{3}}(u') - K_{\frac{2}{3}}(u') \right] (\mathbf{S}_i \cdot \hat{\mathbf{e}}_v)\hat{\mathbf{e}}_v \right\}, \end{aligned} \quad (2)$$

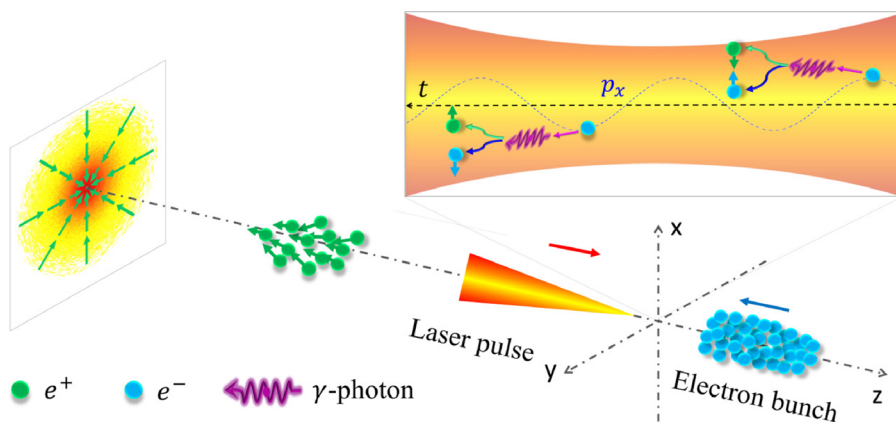


FIG. 1. Scenarios of generating polarized positrons via successive NCS and NBW processes in an ultra-intense laser field. A circularly polarized laser pulse propagating along +z direction head-on colliding with an unpolarized electron bunch produces positrons polarized in radial directions pointing to the center of the beam axis.

$$F_1 = (\mathbf{S}_i \cdot \hat{\mathbf{e}}_1)u(1+u)K_{\frac{1}{3}}(u') + (\mathbf{S}_f \cdot \hat{\mathbf{e}}_1)uK_{\frac{1}{3}}(u') + (\mathbf{S}_f \times \mathbf{S}_i)\hat{\mathbf{e}}_v \left(\frac{u^2}{2} + u \right) K_{\frac{2}{3}}(u') - \frac{u^2}{2} \{ (\mathbf{S}_i \cdot \hat{\mathbf{e}}_1)(\mathbf{S}_f \cdot \hat{\mathbf{e}}_2) + (\mathbf{S}_f \cdot \hat{\mathbf{e}}_1)(\mathbf{S}_i \cdot \hat{\mathbf{e}}_2) \} \text{Int}K_{\frac{1}{3}}(u'), \quad (3)$$

$$F_2 = -(\mathbf{S}_i \cdot \hat{\mathbf{e}}_v)u \text{Int}K_{\frac{1}{3}}(u') - (\mathbf{S}_f \cdot \hat{\mathbf{e}}_v)u(1+u) \text{Int}K_{\frac{1}{3}}(u') + [(\mathbf{S}_i \cdot \hat{\mathbf{e}}_v) + (\mathbf{S}_f \cdot \hat{\mathbf{e}}_v)](2+u)uK_{\frac{2}{3}}(u') - (\mathbf{S}_f \times \mathbf{S}_i)\hat{\mathbf{e}}_1 \left(\frac{u^2}{2} + u \right) K_{\frac{1}{3}}(u') - \frac{u^2}{2} [(\mathbf{S}_i \cdot \hat{\mathbf{e}}_v)(\mathbf{S}_f \cdot \hat{\mathbf{e}}_2) + (\mathbf{S}_f \cdot \hat{\mathbf{e}}_v)(\mathbf{S}_i \cdot \hat{\mathbf{e}}_2)] K_{\frac{1}{3}}(u'), \quad (4)$$

$$F_3 = (1+u)K_{\frac{2}{3}}(u') - u(1+u)(\mathbf{S}_i \cdot \hat{\mathbf{e}}_2)K_{\frac{1}{3}}(u') + (\mathbf{S}_i \cdot \mathbf{S}_f) \times \left(\frac{u^2}{2} + u + 1 \right) K_{\frac{2}{3}}(u') - u(\mathbf{S}_f \cdot \hat{\mathbf{e}}_2)K_{\frac{1}{3}}(u') - \frac{u^2}{2} \{ (\mathbf{S}_i \cdot \hat{\mathbf{e}}_v)(\mathbf{S}_f \cdot \hat{\mathbf{e}}_v)K_{\frac{2}{3}}(u') + [(\mathbf{S}_i \cdot \hat{\mathbf{e}}_1)(\mathbf{S}_f \cdot \hat{\mathbf{e}}_1) - (\mathbf{S}_i \cdot \hat{\mathbf{e}}_2)(\mathbf{S}_f \cdot \hat{\mathbf{e}}_2)] \text{Int}K_{\frac{1}{3}}(u') \}, \quad (5)$$

where $u' = 2u/3\chi_e$, $\text{Int}K_{\frac{1}{3}}(u') \equiv \int_{u'}^{\infty} dz K_{\frac{1}{3}}(z)$, K_n is the n th-order modified Bessel function of the second kind, $\hat{\mathbf{e}}_1$ is the unit vector along the direction of the transverse component of electron acceleration, $\hat{\mathbf{e}}_2 = \hat{\mathbf{e}}_v \times \hat{\mathbf{e}}_1$, where $\hat{\mathbf{e}}_v$ is the unit vector along the electron velocity, and \mathbf{S}_i and \mathbf{S}_f are the electron spin-polarization vectors before and after radiation, respectively, $|\mathbf{S}_{if}| \leq 1$.

When a photon is emitted, its energy is determined by the Monte Carlo algorithm,³¹ and its movement direction is assumed to be along the electron velocity, given the smallness of the emission angle $\sim 1/\gamma_e$ for an ultra-relativistic electron. The Stokes parameter $\boldsymbol{\xi} = (\xi_1, \xi_2, \xi_3)$ for the emitted photon with respect to the axes of $\hat{\mathbf{e}}_1, \hat{\mathbf{e}}_2$ is taken as $\boldsymbol{\xi} = \mathbf{F}/F_0$. The electron final spin is determined by Eq. (1) with photon polarization summed over³⁴

$$\frac{d^2 W_{\text{rad}}}{du dt} = \frac{C_R}{2} (\mathbf{a}_1 + \mathbf{a}_2 \cdot \mathbf{S}_i + \mathbf{b} \cdot \mathbf{S}_f), \quad (6)$$

with

$$\mathbf{a}_1 = -(1+u) \text{Int}K_{\frac{1}{3}}(u') + (u^2 + 2u + 2)K_{\frac{2}{3}}(u'), \quad (7)$$

$$\mathbf{a}_2 = -\hat{\mathbf{e}}_2 u K_{\frac{1}{3}}(u'), \quad (8)$$

$$\mathbf{b} = -(1+u) [\text{Int}K_{\frac{1}{3}}(u') - 2K_{\frac{2}{3}}(u')] \mathbf{S}_i - u(1+u)K_{\frac{1}{3}}(u') \hat{\mathbf{e}}_2 - u^2 [\text{Int}K_{\frac{1}{3}}(u') - K_{\frac{2}{3}}(u')] (\mathbf{S}_i \cdot \hat{\mathbf{e}}_v) \hat{\mathbf{e}}_v. \quad (9)$$

After a photon emission, the electron spin jumps to a mixed state \mathbf{S}_f^R determined by Eq. (1) as

$$\mathbf{S}_f^R = \frac{\mathbf{b}}{\mathbf{a}_1 + \mathbf{a}_2 \cdot \mathbf{S}_i}. \quad (10)$$

If a photon-emission event is rejected, then the electron spin also changes according to the no-emission probability,^{22,32,35} which is explained as the interference of the incoming electron wave function with that of the forward scattered one,³⁶ or in the QED language as radiative correction effect of the one-loop propagator (self-energy).³⁷⁻³⁹

A detailed interpretation of this effect is discussed in Ref. 35. The probability for no-emission reads

$$W_{NR} = \frac{1}{2} (c + \mathbf{S}_f^{NR} \cdot \mathbf{d}), \quad (11)$$

where

$$c = 1 - \int C_R [- (1+u) \text{Int}K_{\frac{1}{3}}(u') + (u^2 + 2u + 2)K_{\frac{2}{3}}(u') - \mathbf{S}_i \cdot \hat{\mathbf{e}}_2 u K_{\frac{1}{3}}(u')] du \Delta t, \quad (12)$$

$$\mathbf{d} = \mathbf{S}_i \left\{ 1 - \int C_R [- (1+u) \text{Int}K_{\frac{1}{3}}(u') + (u^2 + 2u + 2)K_{\frac{2}{3}}(u')] du \Delta t \right\} + \hat{\mathbf{e}}_2 \int C_R u K_{\frac{1}{3}}(u') du \Delta t. \quad (13)$$

The final spin vector of the electron is

$$\mathbf{S}_f^{NR} = \frac{\mathbf{d}}{c}. \quad (14)$$

Similar to the algorithm of photon emission, we use the photon-polarization- and electron (positron)-spin-resolved pair production probability to determine whether a pair is created or not, and then determine the pair's spin states. The pair production probability is²⁷

$$\frac{d^2 W_{\text{pair}}}{d\epsilon_+ dt} = \frac{C_P}{2} (\mathbf{h} + \mathbf{S}_+ \cdot \mathbf{j}), \quad (15)$$

$$\mathbf{h} = \left(\frac{\omega_\gamma^2}{\epsilon_+ \epsilon_-} - 2 \right) K_{\frac{2}{3}}(\rho) + \text{Int}K_{\frac{1}{3}}(\rho) - \xi_3 K_{\frac{1}{3}}(\rho), \quad (16)$$

$$\mathbf{j} = -\xi_1 \frac{\omega_\gamma}{\epsilon_-} K_{\frac{1}{3}}(\rho) \hat{\mathbf{e}}'_1 - K_{\frac{1}{3}}(\rho) \left(\frac{\omega_\gamma}{\epsilon_+} - \xi_3 \frac{\omega_\gamma}{\epsilon_-} \right) \hat{\mathbf{e}}'_2 + \xi_2 \left[\frac{\omega_\gamma}{\epsilon_+} \text{Int}K_{\frac{1}{3}}(\rho) + \frac{\epsilon_+^2 - \epsilon_-^2}{\epsilon_+ \epsilon_-} K_{\frac{2}{3}}(\rho) \right] \hat{\mathbf{e}}'_v, \quad (17)$$

where $C_P = \alpha m^2 / (\sqrt{3} \pi \omega_\gamma)$; $\omega_\gamma, \epsilon_+$, and ϵ_- are the energies of the parent photon, new-born positron, and electron, respectively, with $\omega_\gamma = \epsilon_+ + \epsilon_-$; $\rho = 2\omega_\gamma^2 / (3\chi_\gamma \epsilon_+ \epsilon_-)$; $\boldsymbol{\xi} = (\xi_1, \xi_2, \xi_3)$ refers to the photon polarization vector with ξ_i ($i=1, 2, 3$) the Stokes parameters defined with respect to the axes of $\hat{\mathbf{e}}'_1$ and $\hat{\mathbf{e}}'_2$ [also $\hat{\mathbf{e}}_1$ and $\hat{\mathbf{e}}_2$ in Eq. (1)].¹¹ Note that here $\hat{\mathbf{e}}'_1$ is the unit vector along the direction of the transverse component of positron acceleration, $\hat{\mathbf{e}}'_2 = \hat{\mathbf{e}}'_1 \times \hat{\mathbf{e}}'_v$ with $\hat{\mathbf{e}}'_v$ the unit vector along positron velocity. The spin state of the new-born positron is set as

$$\mathbf{S}_+ = \frac{\mathbf{j}}{h}. \quad (18)$$

The spin state of the new-born electron is also obtained in Eq. (15) by replacing ϵ_+, ϵ_- , and \mathbf{S}_+ with ϵ_-, ϵ_+ , and \mathbf{S}_- , respectively.²⁸

Between quantum events, the electron (positron) dynamics in the ultra-intense laser field are described by Lorentz equations, $d\mathbf{p}/dt = q(\mathbf{E} + \mathbf{v} \times \mathbf{B})$. The spin precession is governed by the Thomas-Bargmann-Michel-Telegdi equation:⁴⁰

$$\frac{d\mathbf{S}}{dt} = \frac{q}{m} \mathbf{S} \times \left[- \left(\frac{g}{2} - 1 \right) \frac{\gamma}{\gamma + 1} (\mathbf{v} \cdot \mathbf{B}) \mathbf{v} + \left(\frac{g}{2} - 1 + \frac{1}{\gamma} \right) \mathbf{B} - \left(\frac{g}{2} - \frac{\gamma}{\gamma + 1} \right) \mathbf{v} \times \mathbf{E} \right], \quad (19)$$

where \mathbf{E} and \mathbf{B} are the laser electric and magnetic fields, respectively, and g is the electron gyromagnetic factor: $g(\chi_e) = 2 + 2\mu(\chi_e)$, $\mu(\chi_e) = \frac{\alpha}{\pi\chi_e} \int_0^\infty \frac{y}{(1+y)^2} \mathbf{L}_\frac{2}{3} \left(\frac{2y}{3\chi_e} \right) dy$, with $\mathbf{L}_\frac{2}{3}(z) = \int_0^\infty \sin \left[\frac{3z}{2} \left(x + \frac{x^3}{3} \right) \right] dx$. As $\chi_e \ll 1$, $g \approx 2.00232$, q is e and $-e$ for electron and positron, respectively.

III. NUMERICAL RESULTS

A typical numerical result for positrons polarization in our scheme is shown in Fig. 2. The peak laser intensity of the circularly polarized tightly focused Gaussian laser pulse⁴¹ is $I_0 \approx 2.5 \times 10^{21}$ W/cm² ($a_0 = 30$), pulse duration (the full width at half maximum) $\tau = 6T_0$ with T_0 being the period at the wavelength of $\lambda = 1\mu$ m, and focal radius $w_0 = 5\lambda$. The electron bunch is considered as a cylindrical form at a length of $L_e = 6\lambda$ and radius of $w_e = 1\lambda$, with $N_e = 1 \times 10^7$ electrons uniformly distributed longitudinally and normally distributed transversely. The initial kinetic energy is 10 GeV, the energy spread is 10%, and the angular divergence is 1 mrad. With the present available laser intensities up to 1×10^{23} W/cm² and electron energy close to 10 GeV (Ref. 42) generated by laser wakefield accelerators and hundreds of GeV by traditional accelerators, we choose the laser and electron parameters above to keep the quantum parameters $\chi_{\gamma,e} > 1$ for substantial high-energy photon emission and pair production. Here, $\chi_{\gamma,e}^{\max} = 4.11$.

The produced positrons concentrate around the center of the angular momentum distribution, and the number density decreases

with the increase in the deflection angles $|\theta_x|$ and $|\theta_y|$, with a total yield of 8.9×10^5 (corresponding to $0.089 e^+/e^-$) [see Fig. 2(a)]. The positrons are polarized radially pointing to the beam-center axis, with the polarization degree increasing with the increase in the deflection angle [see Figs. 2(b) and 2(c)]. The profile curves in Fig. 2(d) show more intuitive features of polarization P_y and the density with respect to the deflection angle. It can be seen that the positrons polarization is opposite for $\pm\theta_y$, respectively, with $P_y > 0$ at $\theta_y > 0$ and $P_y < 0$ at $\theta_y < 0$. Meanwhile, the polarization degree $|P_y|$ increases with the increase in $|\theta_y|$ and the maximum value of $|P_y|$ can be as high as 91%. The average polarization degree is 46.8% for positrons with $\theta_y > 0$ ($\theta_y < 0$), while it is nil for the total positrons due to the symmetric angular distribution of polarization. For experimental applications, it is applicable to utilize post-selection techniques to purify the polarization degree through collecting positrons within a certain angle range. We calculate the polarization of post-selected positrons and their relative fraction as shown in Fig. 3. It can be seen that it is feasible to get a high polarization degree with a sizable positron number proportion. For instance, if we collect positrons within [9.4 mrad, 30 mrad], then corresponding to 1% of the total, we would obtain a polarization of 77%. Higher polarization degree could also be achieved by selecting positrons within a smaller angle range. By collecting the positrons with $\theta_y > 26.5$ mrad, we obtain highly polarized positrons with $P_y > 90\%$, much higher than the existing schemes based on ultra-intense lasers. Indeed, the relative fraction for positrons with polarization $\sim 90\%$ is low. It could still be enhanced by collecting positrons in

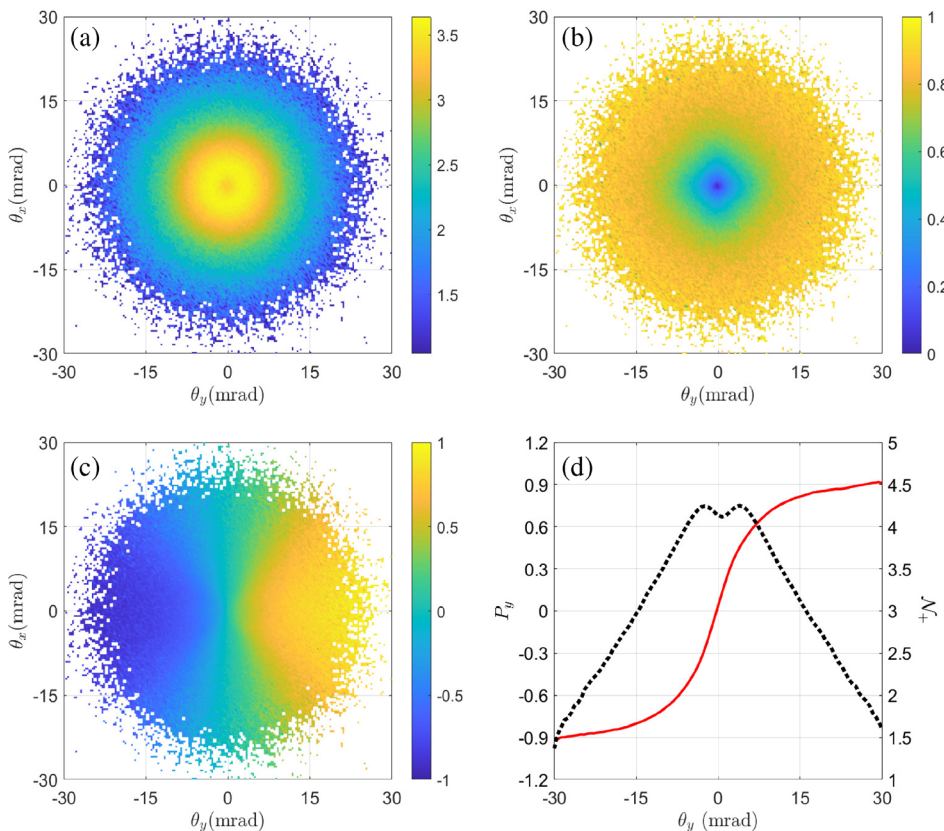


FIG. 2. (a)–(c) Distribution of positron number density $\log [d^2N_{e^+}/(d\theta_x d\theta_y)]$ (mrad⁻²), average transverse polarization degree $|P| = \sqrt{S_x^2 + S_y^2}$, and average polarization in y direction $P_y = \bar{S}_y$ vs deflection angles of $\theta_x = p_x/p_z$ and $\theta_y = p_y/p_z$, respectively. (d) Polarization $P_y = \bar{S}_y$ (red-solid) and positron number density $N_+ = \log_{10}(dN_{e^+}/d\theta_y)$ (mrad⁻¹) (black-dotted) vs θ_y , respectively, with $\theta_x \in [-1.2$ mrad, 1.2 mrad]. The laser and other electron-beam parameters are given in the text.

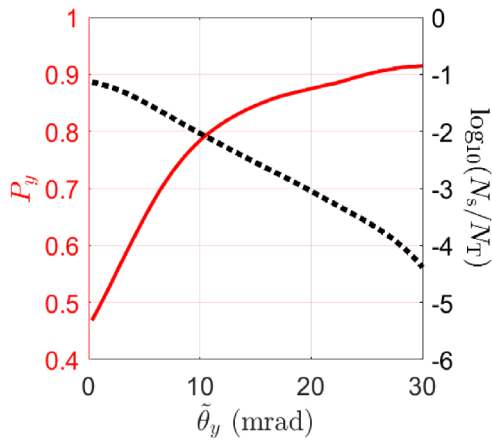


FIG. 3. Polarization P_y of the selected positrons with $\theta_y \in [\tilde{\theta}_y, 30\text{mrad}]$ and $\theta_x \in [-1.2\text{mrad}, 1.2\text{mrad}]$ (left axis) and their relative fraction with respect to the total positron number (right axis) vs the collection angle θ_y .

different radial directions and rotating their polarizations to a same direction via spin-rotators.⁴³ The relatively wide angular distribution of polarization is advantageous for using angle-selection technique to improve the polarization, compared with that in the elliptically polarized laser scheme. The angle-dependent polarization of positrons is connected with their spatial positions. Even though the splitting angle is small (~ 10 mrad), the spatial separation of positrons with different emission angles would be notable after a long propagation distance. For instance, a 10-mrad angle separation corresponds to a 5-cm spatial

separation at a propagation distance of 5 m. Therefore, the positrons with different spins are well-separated in space and can be split.

The reasons for the production of highly polarized positrons are elucidated in Figs. 4 and 5. Two typical QED processes in strong fields are: the emission of photons by electrons by NCS, and the production of pairs by high-energy photons via the NBW process. Let us start with the photon-emission process during NCS. The angular distribution of the photons emitted during the NCS process is shown in Fig. 4. The high-energy photons are well collimated with a small polar angle range within 3 mrad [see Fig. 4(a)]. The angular spread of photons is one order of magnitude less than that of the positrons in Fig. 2, indicating that the contribution of parent γ -photons to the final transverse momentum of positrons is negligible. From Figs. 4(b)–4(d), it can be seen that the photons are transversely polarized as $\xi_2 \approx 0$, and $\xi_{1,3}$ (ranging from -0.6 to 0.6) centrosymmetrically distributed around the beam-center axis. For the whole photon beam, the average polarization becomes zero due to the cancelation from different parts of the beam.

Let us proceed to the analysis of the angle-dependent polarization of positrons generated during NBW. The final transverse momentum of a positron can be estimated as $\mathbf{P}_\perp^f \approx \mathbf{P}_\perp^i - e\mathbf{A}(\eta_+)$, where \mathbf{P}_\perp^i is the momentum inherited from the parent photon, and $\mathbf{A}(\eta_+)$ is the vector potential at the creation point with $\eta_+ = \omega_0 t_+ - k_0 z_+$ being the creation phase of the pairs. Comparing the angular distribution of Figs. 2 and 4, it is clear that $\mathbf{P}_\perp^i \ll \mathbf{P}_\perp^f$ and consequently $\mathbf{P}_\perp^f \approx -e\mathbf{A}(\eta_+)$, indicating that the final transverse momentum of a positron is determined by the laser field where the positron is created. From Eqs. (15)–(18), the spin state of a positron at the creation phase can be derived as

$$\mathbf{S}_+ = \frac{-\xi_1 \frac{\omega_\gamma}{\varepsilon_-} \mathbf{K}_3(\rho) \hat{\mathbf{e}}_1 - \left(\frac{\omega_\gamma}{\varepsilon_+} - \xi_3 \frac{\omega_\gamma}{\varepsilon_+} \right) \mathbf{K}_3(\rho) \hat{\mathbf{e}}_2 + \xi_2 \left[\frac{\omega_\gamma}{\varepsilon_+} \text{IntK}_3(\rho) + \frac{\varepsilon_+^2 - \varepsilon_-^2}{\varepsilon_+ \varepsilon_-} \mathbf{K}_3(\rho) \right] \hat{\mathbf{e}}_v}{\left(\frac{\omega_\gamma^2}{\varepsilon_+ \varepsilon_-} - 2 \right) \mathbf{K}_3(\rho) + \text{IntK}_3(\rho) - \xi_3 \mathbf{K}_3(\rho)}. \tag{20}$$

In the case $\xi_{1,2,3} \approx 0$, one obtains

$$\mathbf{S}_+ = \frac{-\left(\frac{\omega_\gamma}{\varepsilon_+} \right) \mathbf{K}_3(\rho) \hat{\mathbf{e}}_2}{\left(\frac{\omega_\gamma^2}{\varepsilon_+ \varepsilon_-} - 2 \right) \mathbf{K}_3(\rho) + \text{IntK}_3(\rho)}. \tag{21}$$

Equation (21) shows that the created positron is polarized anti-parallel to $\hat{\mathbf{e}}_2$, which is roughly the opposite direction of the instantaneous magnetic field at η_+ . In a circularly polarized laser field, the magnetic field is parallel with $-\mathbf{A}(\eta_+)$ for arbitrary η_+ and, consequently, $-\mathbf{P}_\perp^f \parallel \mathbf{S}_+(\eta_+)$ with $\mathbf{S}_+(\eta_+)$ being the polarization of the positron at the creation phase. Thus, $\theta \approx -\mathbf{P}_\perp^f / \gamma_e \parallel \mathbf{S}_+(\eta_+)$. The positrons could undergo radiation reaction effect in the laser field, which may break the correlation between polarization and final transverse momentum built when the pair is created. However, thanks to the moderate laser

intensity employed in our scheme, the influence of radiation reaction effect on the angular distribution of polarization is negligible (see Fig. 5). Therefore, the positrons keep radically polarized even after moving out of the laser field.

The correlation between polarization degree and deflection angle θ is explained below, by means of the relation of polarization S_+ and pair-production probability with respect to the energy ratio $\varepsilon_+/\omega_\gamma$ as illustrated in Fig. 6. The dependence of polarization and probability on the positron energy $\varepsilon_+/\omega_\gamma$ are plotted for $\chi_\gamma = 1.7$ and 4.1 , which are the maximum and average value of χ_γ , respectively. In both the cases, the positron spin component S_+ decreases from 1 to 0, as $\varepsilon_+/\omega_\gamma$ increases from 0 to 1 [see Fig. 6(a)], with a wide energy spectrum, ranging from 0 to ω_γ [see Fig. 6(b)]. It results in that the positrons with lower energies tend to show larger deflection angles $\theta \sim |\mathbf{P}_\perp^f| m / \varepsilon_+ \propto 1/\varepsilon_+$ and higher polarization. In addition, for the low energy part, i.e., $\varepsilon_+ \sim 0$, the positron polarization could be close to 1. However, it is hard to get 100% polarized positrons in a realistic

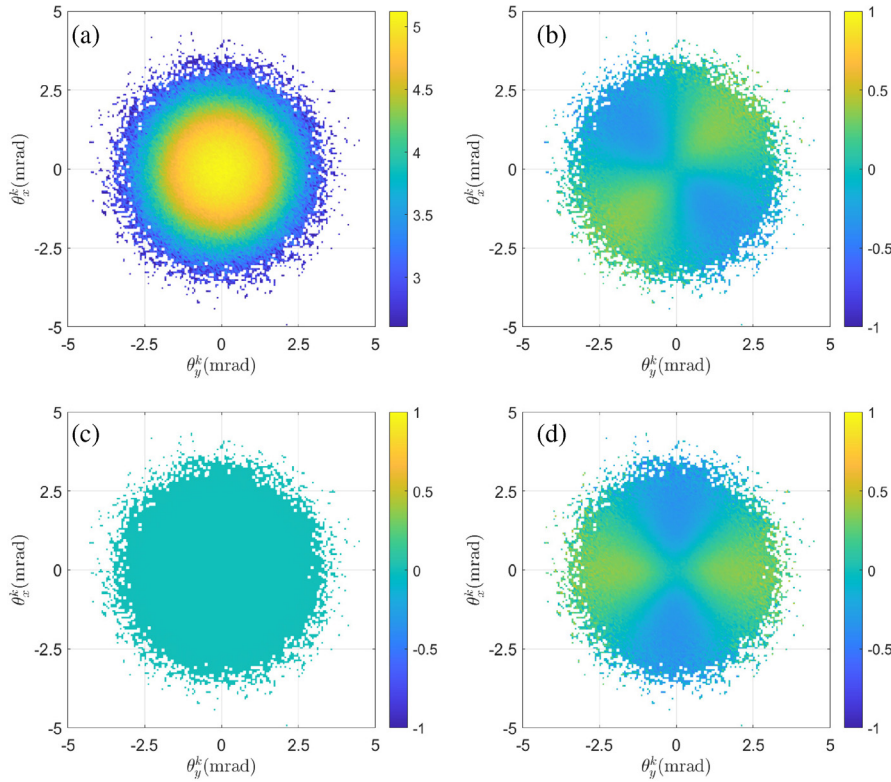


FIG. 4. Distribution of number density $\log [d^2N_\gamma/(d\theta_x^k d\theta_y^k)]$ (mrad^{-2}) (a) and three components of the Stokes vectors $\xi = (\xi_1, \xi_2, \xi_3)$ (b)–(d) of the photons emitted during NCS vs the photon deflection angles $\theta_x^k = k_x/k_z$ and $\theta_y^k = k_y/k_z$, respectively.

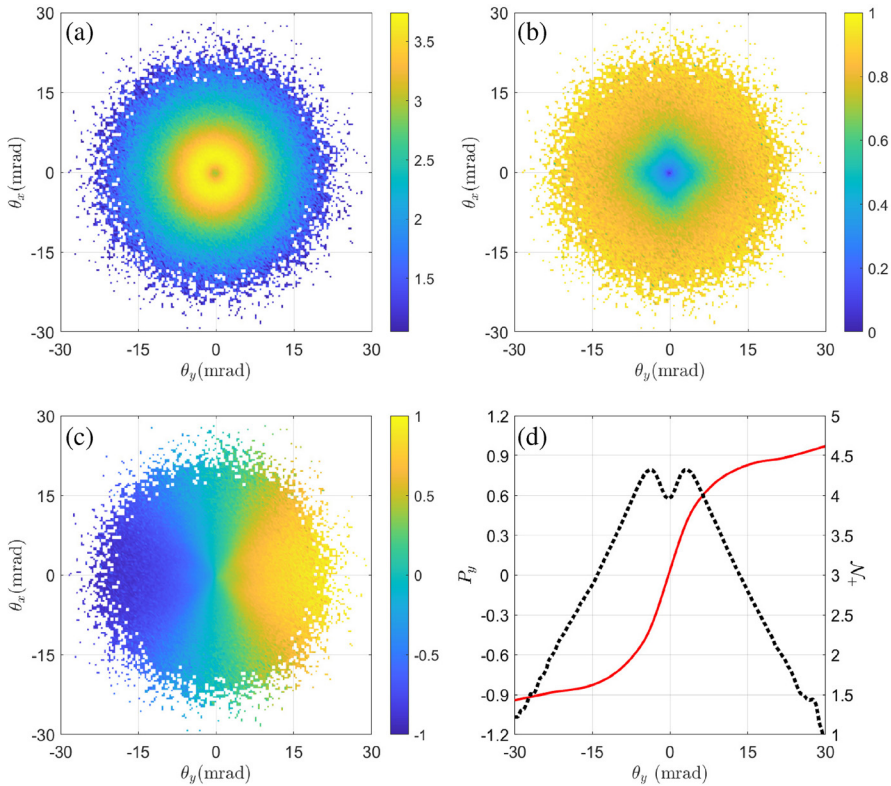


FIG. 5. Simulation results of positron distributions with positron radiation effect is removed artificially. (a)–(c) Distribution of positron number density $\log [d^2N_{e^+}/(d\theta_x d\theta_y)]$ (mrad^{-2}), average transverse polarization degree $|P_\perp|$, and P_y vs the deflection angles θ_x and θ_y , respectively. (d) Polarization P_y (red-solid) and positron number density $N_+ = \log_{10}(dN_{e^+}/d\theta_y)$ (mrad^{-1}) (black-dotted) vs θ_y , respectively, with $\theta_x \in [-1.2 \text{ mrad}, 1.2 \text{ mrad}]$. The laser and other electron-beam parameters are the same as those in Fig. 2.

07 September 2023 12:31:44

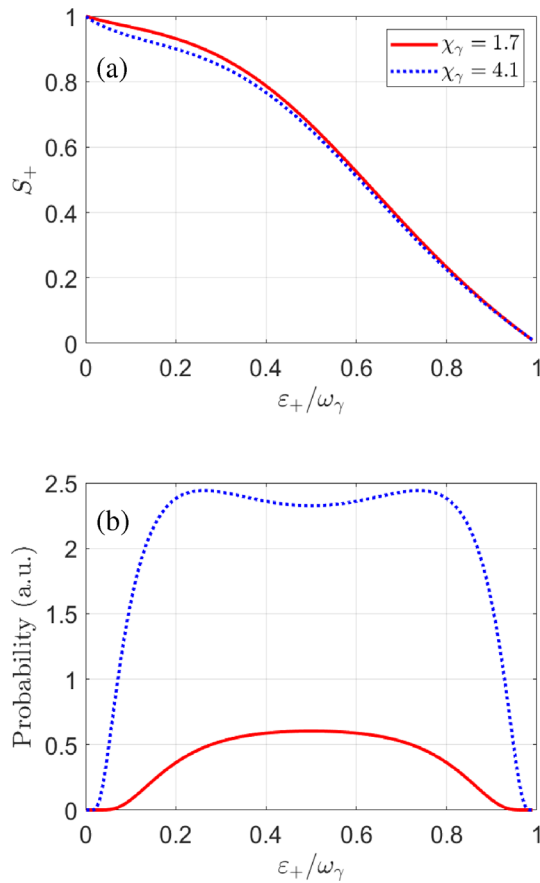


FIG. 6. Positron spin S_+ (a) and pair-production probability (b) calculated by Eqs. (21) and (15) vs the energy ratio $\varepsilon_+/\omega_\gamma$, with $\chi_\gamma = 1.7$ (red-solid) and 4.1 (blue-dotted), respectively.

scenario (Fig. 2), due to the overlapping of positrons with different energies but with the same deflection angles.

The polarization schemes employing linearly or elliptically polarized lasers perform badly in obtaining highly polarized positrons. In the former case, the kinetic motion of particles is roughly in the x - z plane, resulting in a negligible angular spread over θ_y [Fig. 7(a)]. With the quantization axis along the magnetic field direction, $S_x = 0$ is obtained [see Fig. 7(b)]. In the laser field, the magnetic field B_y has a $\pi/2$ phase delay with respect to vector potential A_x . The positrons created at $B_y > 0$ and $S_y > 0$ ($B_y < 0$ and $S_y < 0$) could have final momentum $P_x^f > 0$ or $P_x^f < 0$. Consequently, the created positrons with $S_y > 0$ or $S_y < 0$ are mixed together, resulting in an unpolarized beam ($P_y = 0$) [see Fig. 7(b)].

The elliptically polarized laser cases are discussed in detail in Refs. 21 and 24. To ensure a sufficient deflection angle for post-selection, one has to employ lasers with high intensities. The typical amplitudes along major and minor axes of the ellipse are $a_x \approx 100$ and $a_y \approx 10$, respectively, corresponding to a laser intensity of $\approx 10^{22}$ W/cm². Such a high laser intensity would enhance the depolarization effect for positrons due to the radiation recoil effect.²¹ In addition, the influence of photon polarization ($\xi_3 \sim 0.5$) in positron

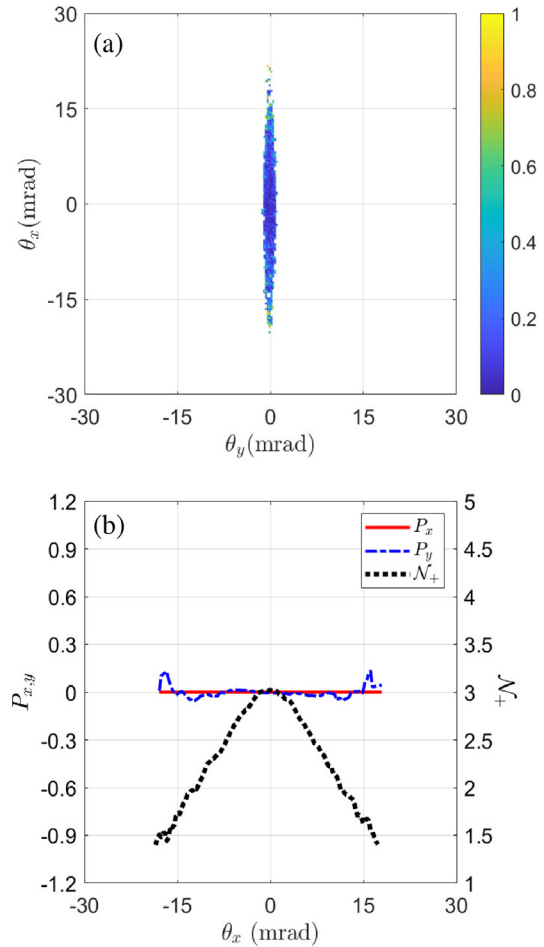


FIG. 7. Simulation result of the laser-electron interaction with a linearly polarized (along x axis) laser pulse. (a) Average transverse polarization degree $|P|$ vs the deflection angles θ_x and θ_y , respectively. (b) Polarization $P_x = S_x$ (red-solid), $P_y = S_y$ (blue-dashed-dotted) and positron-number density $N_+ = \log_{10}(dN_{e+}/d\theta_x)$ (black-dotted) vs θ_x . The other laser and electron-beam parameters are the same as those in Fig. 2.

polarization is not trivial, causing the average polarization to be degraded by 35%.²⁴

The impacts of laser and electron-beam parameters on the positron polarization are studied in Fig. 8. When the laser intensity a_0 increases from 20 to 40, the gradient of the curve declines due to $\theta \propto a_0$ [see Fig. 8(a)]. The maximum polarization degree for $a_0 = 20$ and $a_0 = 30$ are similar, but reduces to 84% for $a_0 = 40$ due to the nontrivial radiation reaction. The polarization curve remains stable when the laser pulse duration changes from $4T_0$ to $8T_0$, except for a more intense fluctuation appearing at large θ_y region for shorter τ [see Fig. 8(b)]. The fluctuation arises due to the reduction in the positron yield. The polarization degree is proportional to the initial seed electron energy [see Fig. 8(c)]. For a certain deflection angle, $\theta_y \propto 1/\varepsilon_+$, the larger ε_0 corresponds to lower energy ratio $\varepsilon_+/\omega_\gamma$ as $\omega_\gamma \propto \varepsilon_0$ and larger polarization as shown in Fig. 6(a). Thus, larger ε_0 is preferred

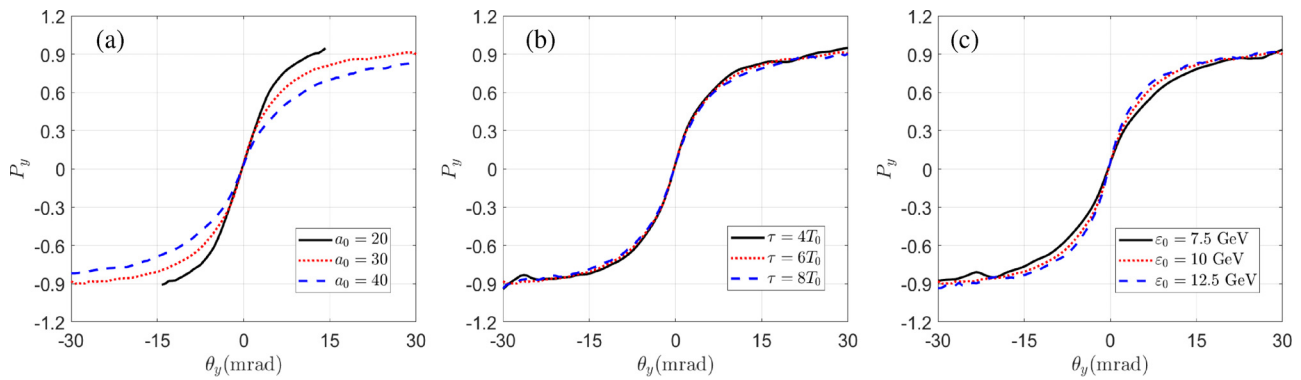


FIG. 8. Impacts of laser and electron-beam parameters, including laser intensity (a), pulse duration (b) and initial seed-electron energy (c), on the positron polarization.

for higher polarization and positron yield but it cannot be too large for the suppression of the radiation reaction effect.

Conclusively, we have investigated the production of highly polarized positrons via successive nonlinear Compton scattering and nonlinear Breit–Wheeler processes during the interaction between a circularly polarized few-PW laser pulse and an ultra-relativistic electron beam. Taking advantage of the correlation of the final momentum and the polarization of the positron created in a circularly polarized field and the suppression of the depolarization effect originating from radiation recoils, the positron polarization can reach up to 91% with a laser intensity of $\sim 10^{21}$ W/cm². Compared with the existing schemes of producing polarized positrons with lasers, our scheme provides the highest polarization degree but with the lowest laser intensity, which makes it an attractive method for preparing highly polarized positrons in a femtosecond timescale. The highly polarized positrons could be used for applications, such as experiments in high-energy physics, nuclear physics, and material physics.

ACKNOWLEDGMENTS

This work was supported by the National Natural Science Foundation of China (Grant Nos. 12075187, 12074262, and 12222507), and the Strategic Priority Research Program of Chinese Academy of Sciences (Grant No. XDA25031000).

AUTHOR DECLARATIONS

Conflict of Interest

The authors have no conflicts to disclose.

Author Contributions

Bing-Jun Li: Data curation (lead); Formal analysis (equal); Investigation (lead); Methodology (equal); Writing – original draft (equal). **Yanfei Li:** Conceptualization (lead); Formal analysis (equal); Funding acquisition (equal); Methodology (equal); Project administration (lead); Supervision (equal); Writing – original draft (equal); Writing – review & editing (lead). **Yue-Yue Chen:** Conceptualization (supporting); Formal analysis (equal); Investigation (equal); Validation (equal); Project administration (equal); Writing – original draft (equal); Writing – review & editing (equal). **Xiufeng Weng:** Data curation (equal); Formal analysis (equal). **Xinjian Tan:** Conceptualization

(supporting); Investigation (equal); Supervision (supporting). **Xinjie Ma:** Data curation (supporting); Formal analysis (supporting); Investigation (supporting). **Liang Sheng:** Funding acquisition (supporting); Supervision (equal). **Huasi Hu:** Funding acquisition (equal); Project administration (equal); Supervision (lead).

DATA AVAILABILITY

The data that support the findings of this study are available from the corresponding author upon reasonable request.

REFERENCES

- ¹L. Elouadrhiri, T. A. Forest, J. Grames, W. Melnitchouk, and E. Voutier, in *Proceedings of the International Workshop on Positrons at Jefferson Lab, AIP Conference Proceedings* (AIP, 2009), Vol. 1160.
- ²A. V. Subashiev, Yu. A. Mamaev, Yu. P. Yashin, and J. E. Clendenin, “Spin polarized electrons: Generation and applications,” *Phys. Low Dimens. Struct.* **1**, 1 (1998), [SLAC PUB 8035 (1998)]; available at <https://www-public.slac.stanford.edu/sciDoc/docMeta.aspx?slacPubNumber=SLAC-PUB-8035>.
- ³G. Moortgat-Pick, T. Abe, G. Alexander, B. Ananthanarayan, A. A. Babich, V. Bharadwaj, D. Barber, A. Bartl, A. Brachmann, S. Chen, J. Clarke, J. E. Clendenin, J. Dainton, K. Desch, M. Diehl, B. Dobos, T. Dorland, H. K. Dreiner, H. Eberl, J. Ellis, K. Flöttmann, H. Fraas, F. Franco-Solova, F. Franke, A. Freitas, J. Goodson, J. Gray, A. Han, S. Heinemeyer, S. Hesselbach, T. Hirose, K. Hohenwarter-Sodek, A. Juste, J. Kalinowski, T. Kernreiter, O. Kittel, S. Kraml, U. Langenfeld, W. Majerotto, A. Martinez, H.-U. Martyn, A. Mikhailichenko, C. Milstene, W. Menges, N. Meyners, K. Mönig, K. Moffeit, S. Moretti, O. Nachtmann, F. Nagel, T. Nakanishi, U. Nauenberg, H. Nowak, T. Omori, P. Osland, A. A. Pankov, N. Paver, R. Pitthan, R. Pöschl, W. Porod, J. Proulx, P. Richardson, S. Riemann, S. D. Rindani, T. G. Rizzo, A. Schällicke, P. Schüler, C. Schwanenberger, D. Scott, J. Sheppard, R. K. Singh, A. Sopczak, H. Spiesberger, A. Stahl, H. Steiner, A. Wagner, A. M. Weber, G. Weiglein, G. W. Wilson, M. Woods, P. Zerwas, J. Zhang, and F. Zomer, “Polarized positrons and electrons at the linear collider,” *Phys. Rep.* **460**, 131–243 (2008).
- ⁴D. W. Gidley, A. R. Köymen, and T. Weston Capehart, “Polarized low-energy positrons: A new probe of surface magnetism,” *Phys. Rev. Lett.* **49**, 1779–1783 (1982).
- ⁵J. Van House and P. W. Zitzewitz, “Probing the positron moderation process using high-intensity, highly polarized slow-positron beams,” *Phys. Rev. A* **29**, 96–105 (1984).
- ⁶A. A. Sokolov and I. M. Ternov, “On polarization and spin effects in the theory of synchrotron radiation,” *Sov. Phys. Dokl.* **8**, 1203 (1964).
- ⁷P. W. Zitzewitz, J. C. Van House, A. Rich, and D. W. Gidley, “Spin polarization of low-energy positron beams,” *Phys. Rev. Lett.* **43**, 1281–1284 (1979).
- ⁸T. Behnke, J. E. Brau, B. Foster, J. Fuster, M. Harrison, J. M. Paterson, M. Peskin, M. Stanitzki, N. Walker, and H. Yamamoto, “The international linear

- collider technical design report - volume 1: Executive summary," [arXiv:1306.6327](https://arxiv.org/abs/1306.6327) (2013).
- ⁹H. Aihara, J. Bagger, P. Bambade, B. Barish, T. Behnke, A. Bellerive, M. Berggren, J. Brau, M. Breidenbach, I. Bozovic-Jelisavcic *et al.*, "The international linear collider. A global project," [arXiv:1901.09829](https://arxiv.org/abs/1901.09829) (2019).
- ¹⁰A. P. Potylitsin, "Production of polarized positrons through interaction of longitudinally polarized electrons with thin targets," *Nucl. Instrum. Methods Phys. Res., Sect. A* **398**, 395–398 (1997).
- ¹¹W. H. McMaster, "Matrix representation of polarization," *Rev. Mod. Phys.* **33**, 8–28 (1961).
- ¹²V. A. Baskov, "Radiation length of the oriented crystal," *Bull. Lebedev Phys. Inst.* **42**, 144 (2015).
- ¹³D. Abbott, P. Adderley, A. Adeyemi, P. Aguilera, M. Ali, H. Areti, M. Baylac, J. Benesch, G. Bosson, B. Cade, A. Camsonne, L. S. Cardman, J. Clark, P. Cole, S. Covert, C. Cuevas, O. Dadoun, D. Dale, H. Dong, J. Dumas, E. Fanchini, T. Forest, E. Forman, A. Freyberger, E. Froidefond, S. Golge, J. Grames, P. Guéye, J. Hansknecht, P. Harrell, J. Hoskins, C. Hyde, B. Josey, R. Kazimi, Y. Kim, D. Machie, K. Mahoney, R. Mammei, M. Marton, J. McCarter, M. McCaughan, M. McHugh, D. McNulty, K. E. Mesick, T. Michaelides, R. Michaels, B. Moffit, D. Moser, C. Muñoz Camacho, J.-F. Muraz, A. Oppen, M. Poelker, J.-S. Réal, L. Richardson, S. Setiniyaz, M. Stutzman, R. Suleiman, C. Tennant, C. Tsai, D. Turner, M. Ungaro, A. Variola, E. Voutier, Y. Wang, Y. Zhang, and PEPPO Collaboration, "Production of highly polarized positrons using polarized electrons at MEV energies," *Phys. Rev. Lett.* **116**, 214801 (2016).
- ¹⁴H. Olsen and L. C. Maximon, "Photon and electron polarization in high-energy bremsstrahlung and pair production with screening," *Phys. Rev.* **114**, 887–904 (1959).
- ¹⁵J. C. Liu, T. Kotseroglou, W. R. Nelson, and D. Schultz, "Polarization study for NLC positron source using EGS4," Report No. SLAC-PUB-8477 (2000).
- ¹⁶T. Omori, M. Fukuda, T. Hirose, Y. Kurihara, R. Kuroda, M. Nomura, A. Ohashi, T. Okugi, K. Sakaue, T. Saito, J. Urakawa, M. Washio, and I. Yamazaki, "Efficient propagation of polarization from laser photons to positrons through Compton scattering and electron-positron pair creation," *Phys. Rev. Lett.* **96**, 114801 (2006).
- ¹⁷G. Alexander, J. Barley, Y. Batygin, S. Berridge, V. Bharadwaj, G. Bower, W. Bugg, F.-J. Decker, R. Dollan, Y. Efremenko, V. Gharibyan, C. Hast, R. Iverson, H. Kolanoski, J. Kovermann, K. Laihem, T. Lohse, K. T. McDonald, A. A. Mikhailichenko, G. A. Moortgat-Pick, P. Pahl, R. Pitthan, R. Pöschl, E. Reinherz-Aronis, S. Riemann, A. Schälicke, K. P. Schüler, T. Schweizer, D. Scott, J. C. Sheppard, A. Stahl, Z. M. Szalata, D. Walz, and A. W. Weidemann, "Observation of polarized positrons from an undulator-based source," *Phys. Rev. Lett.* **100**, 210801 (2008).
- ¹⁸K. Flottman, "Investigations toward the development of polarized and unpolarized high intensity positron sources for linear colliders," Report No. DESY 93-161 (1993).
- ¹⁹T. Omori, T. Takahashi, S. Riemann, W. Gai, J. Gao, S. I. Kawada, W. Liu, N. Okuda, G. Pei, J. Urakawa, and A. Ushakov, "A conventional positron source for international linear collider," *Nucl. Instrum. Methods Phys. Res., Sect. A* **672**, 52–56 (2012).
- ²⁰Y.-Y. Chen, P.-L. He, R. Shaisultanov, K. Z. Hatsagortsyan, and C. H. Keitel, "Polarized positron beams via intense two-color laser pulses," *Phys. Rev. Lett.* **123**, 174801 (2019).
- ²¹F. Wan, R. Shaisultanov, Y.-F. Li, K. Z. Hatsagortsyan, C. H. Keitel, and J.-X. Li, "Ultrarelativistic polarized positron jets via collision of electron and ultraintense laser beams," *Phys. Lett. B* **800**, 135120 (2020).
- ²²Y.-F. Li, Y.-Y. Chen, W.-M. Wang, and H.-S. Hu, "Production of highly polarized positron beams via helicity transfer from polarized electrons in a strong laser field," *Phys. Rev. Lett.* **125**, 044802 (2020).
- ²³H.-H. Song, W.-M. Wang, and Y.-T. Li, "Generation of polarized positron beams via collisions of ultrarelativistic electron beams," *Phys. Rev. Res.* **3**, 033245 (2021).
- ²⁴Y.-N. Dai, B.-F. Shen, J.-X. Li, R. Shaisultanov, K. Z. Hatsagortsyan, C. H. Keitel, and Y.-Y. Chen, "Photon polarization effects in polarized electron-positron pair production in a strong laser field," *Matter Radiat. Extremes* **7**, 014401 (2022).
- ²⁵C. Sun, J. Zhang, J. Li, W. Z. Wu, S. F. Mikhailov, V. G. Popov, H. L. Xu, A. W. Chao, and Y. K. Wu, "Polarization measurement of stored electron beam using Touschek lifetime," *Nucl. Instrum. Methods Phys. Res., Sect. A* **614**, 339–344 (2010).
- ²⁶V. I. Ritus, "Quantum effects of the interaction of elementary particles with an intense electromagnetic field," *J. Sov. Laser Res.* **6**, 497 (1985).
- ²⁷V. N. Baier, V. M. Katkov, and V. M. Strakhovenko, *Electromagnetic Processes at High Energies in Oriented Single Crystals* (World Scientific, Singapore, 1998).
- ²⁸Y.-Y. Chen, K. Z. Hatsagortsyan, C. H. Keitel, and R. Shaisultanov, "Electron spin- and photon polarization-resolved probabilities of strong-field QED processes," *Phys. Rev. D* **105**, 116013 (2022).
- ²⁹C. P. Ridgers, J. G. Kirk, R. Ducloux, T. G. Blackburn, C. S. Brady, K. Bennett, T. D. Arber, and A. R. Bell, "Modelling gamma-ray photon emission and pair production in high-intensity laser-matter interactions," *J. Comput. Phys.* **260**, 273–285 (2014).
- ³⁰N. V. Elkina, A. M. Fedotov, I. Y. Kostyukov, M. V. Legkov, N. B. Narozhny, E. N. Nerush, and H. Ruhl, "QED cascades induced by circularly polarized laser fields," *Phys. Rev. ST Accel. Beams* **14**, 054401 (2011).
- ³¹A. Gonoskov, S. Bastrakov, E. Efimenko, A. Ilderton, M. Marklund, I. Meyerov, A. Muraviev, A. Sergeev, I. Surmin, and E. Wallin, "Extended particle-in-cell schemes for physics in ultrastrong laser fields: Review and developments," *Phys. Rev. E* **92**, 023305 (2015).
- ³²See <https://www.jlc.kek.jp/subg/ir/lib/cain21b.manual/> for "User's Manual of CAIN" (access date December 1, 2022).
- ³³Y.-F. Li, R. Shaisultanov, Y.-Y. Chen, F. Wan, K. Z. Hatsagortsyan, C. H. Keitel, and J.-X. Li, "Polarized ultrashort brilliant multi-GeV γ rays via single-shot laser-electron interaction," *Phys. Rev. Lett.* **124**, 014801 (2020).
- ³⁴Y.-F. Li, R. Shaisultanov, K. Z. Hatsagortsyan, F. Wan, C. H. Keitel, and J.-X. Li, "Ultrarelativistic electron-beam polarization in single-shot interaction with an ultraintense laser pulse," *Phys. Rev. Lett.* **122**, 154801 (2019).
- ³⁵Y.-F. Li, Y.-Y. Chen, K. Z. Hatsagortsyan, A. Di Piazza, M. Tamburini, and C. H. Keitel, "Strong signature of one-loop self-energy in polarization resolved nonlinear Compton scattering," *Phys. Rev. D* **107**, 116020 (2023).
- ³⁶G. L. Kotkin, H. Perl, and V. G. Serbo, "Polarization of high-energy electrons traversing a laser beam," *Nucl. Instrum. Methods Phys. Res. Sect. A* **404**, 430–436 (1998).
- ³⁷S. Meuren and A. Di Piazza, "Quantum electron self-interaction in a strong laser field," *Phys. Rev. Lett.* **107**, 260401 (2011).
- ³⁸A. Ilderton, B. King, and S. Tang, "Loop spin effects in intense background fields," *Phys. Rev. D* **102**, 076013 (2020).
- ³⁹G. Torgrimsson, "Loops and polarization in strong-field QED," *New J. Phys.* **23**, 065001 (2021).
- ⁴⁰V. Bargmann, L. Michel, and V. L. Telegdi, "Precession of the polarization of particles moving in a homogeneous electromagnetic field," *Phys. Rev. Lett.* **2**, 435–436 (1959).
- ⁴¹Y. I. Salamin, G. R. Mocken, and C. H. Keitel, "Electron scattering and acceleration by a tightly focused laser beam," *Phys. Rev. ST Accel. Beams* **5**, 101301 (2002).
- ⁴²A. J. Gonsalves, K. Nakamura, J. Daniels, C. Benedetti, C. Pieronek, T. C. H. de Raadt, S. Steinke, J. H. Bin, S. S. Bulanov, J. van Tilborg, C. G. R. Geddes, C. B. Schroeder, C. Tóth, E. Esarey, K. Swanson, L. Fan-Chiang, G. Bagdasarov, N. Bobrova, V. Gasilov, G. Korn, P. Satorov, and W. P. Leemans, "Petawatt laser guiding and electron beam acceleration to 8 GeV in a laser-heated capillary discharge waveguide," *Phys. Rev. Lett.* **122**, 084801 (2019).
- ⁴³J. Buon and K. Steffen, "Hera variable-energy 'mini' spin rotator and head-on ep collision scheme with choice of electron helicity," *Nucl. Instrum. Methods Phys. Res., Sect. A* **245**, 248–261 (1986).